Multilayer Needle Insertion Modeling for Robotic Percutaneous Therapy

Alexandre Carra and Juan Carlos Avila-Vilchis
Universidad Autónoma del Estado de México, Facultad de Ingeniería
50000 Toluca, Estado de México, Mexico
carraalex@gmail.com

***Abstract*—The modeling of needle insertion into tissues is important for simulation of this procedure and for robotic technologies applied to percutaneous therapy. In this article, we present a first attempt to develop a general force model for the needle insertion throw different tissue layers (skin, fat and muscle) to reach an internal organ (the liver, for instance) with objectives of control, looking for an optimal (less invasive and more accurate) puncture task. The forces are divided into three parts: stiffness, a nonlinear model; friction, a modified Dahl model; and cutting, a constant for a given tissue. Results show that the overall shape of forces presents the main phases of a needle insertion through several tissue layers.**

Keywords-component; percutaneous therapy; modeling; robotic; multilayer

I. INTRODUCTION

Many modern clinical practices involve percutaneous needle insertions. In these procedures, thin needles have to be inserted deep into the human body to reach a target. Usually, target visibility, target access and tool maneuverability in addition to physiological changes of the target are key issues. During some conventional needle insertion procedures, the surgeon relies on kinesthetic feedback from the needle and his or her mental 3D visualization of the anatomical structure. However, targeting error (needle misplacement) can occur due to imaging limitations, target uncertainty, human errors, tissue deformation and/or needle deflection. Robotics and imaging technologies have become important aids to assist medical personnel in percutaneous therapy. The robotic systems reduce trauma to patients, ease the task of surgeons and provide better treatments. However, there are a few issues to be addressed such as the change of behavior of the needle when it goes through different tissue layers.

A. Needle Insertion Modeling

The modeling of forces involved in percutaneous needle insertion into the human body is important for accurate surgical simulation or robot-assisted medical procedures. In this context, numerous studies have been proposed and a state-of-the-art of the domain recently appeared [1]. The different works can be classified into two categories according to the data acquisition: artificial phantoms and animal tissues.

In the first category, DiMaio et al. [2] studied the correlation between forces and deformations. Crouch et al. [3] focused on the dynamical effects of needle insertion whereas Dehghan et al. [4] presented a force model for needle-tissue interaction based on the tissue displacement estimates and the recorded insertion force. Such studies mainly are motivated by the development of simulators to help clinicians.

In the second category, Kataoka et al. [5] quantified the tip and friction forces of a needle on penetration into the prostate of a canine cadaver. In [6], Okamura et al. demonstrated that the force between tissues and the needle is a summation of stiffness, friction and cutting forces. Nevertheless, these experiences deal with dead tissues which rheological properties are a little altered. To compensate this problem, some studies are carried out using *in vivo* tissues. Brouwer et al. [7] and Brown et al. [8] developed devices to measure tissue properties. Maurin et al. [9] used different conditions and different organs to characterize the forces involved in *in vivo* percutaneous procedures. Recently, Barbé et al. [10] proposed a force model from measurable information in operating conditions. However, to the best of our knowledge, there are not works taking into account the insertion of a needle through several tissue layers where the dynamic of each layer is considered as a part of a general model.

B. Contributions and Outline

The main contribution of this paper is the synthesis of a general force model for the needle insertion throw the skin, the fat and the muscle to finally reach the liver. This model synthesis is performed with objectives of control, looking for an optimal (less invasive and more accurate) puncture task. The liver concerns the organ of interest due to its relevance to important percutaneous procedures. For instance, liver biopsy involves the insertion of a biopsy needle to retrieve a tissue sample. It is often used to diagnose the cause and extent of chronic liver disease and diagnose liver tumors identified by imaging tests. In section 2, the model of forces is presented. Section 3 is dedicated to simulations of this procedure using the multilayer needle insertion model. Finally, we will summarize the main contribution of this work and talk about future work.

II. NEEDLE INSERTION FORCES

In order to accurately model the forces resulting from needle insertion, it is necessary to separate force data into components. Okamura et al. [6] have demonstrated that forces

This work is supported by the Mexican SRE (Secretaría de Relaciones Exteriores) and the French Ministry of Foreign and European Affairs.

between tissues and needles are composed of stiffness, friction and cutting forces**.** Then, the force *F(x)* acting on a needle is written as:

$$F(x) = f_s(x) + f_f(x) + f_c(x) \quad (1)$$

where x is the position of the needle tip relative to a fixed coordinate system before puncture, f_s, f_f and f_c are, respectively, the stiffness force, the friction force and the cutting force.

A. Stiffnesse Force

The stiffness force corresponds to a viscoelastic interaction as described by Fung [11] and can be identified as pre-puncture force. In this case, the needle is not longer cutting the tissue but is instead compressing it until the tip force reached the magnitude required for puncturing the surface membrane [12]. Barbé et al. [10] proved that the Hunt-Crossley model well matches this deformation. It states that the interaction model varies in a nonlinear way regardless of the tissue motion as in (2).

$$f_s = \begin{cases} 0 & x \le d_i \\ \mu x^n + \lambda x^n \dot{x} & d_i < x \le d_j \\ 0 & x > d_j \end{cases} \quad (2)$$

where $\dot{x}$ represents the velocity of the needle tip; d_i, d_j are the positions of the tissue surface relative to a fixed coordinate system. μ, λ and n are constant parameters that depend on the material properties.

Remark**.** As the needle-tip speed is constant (or relatively slow that it may be neglected), the stiffness force f_s will be just described as $f_s \approx \mu x^n$.

B. Friction Force

The friction force occurs along the length of the needle inside the tissue and is due to Coulomb friction, tissue adhesion and damping. Friction is a natural phenomenon that is quite hard to model and it is not yet completely understood. However, an important number of works can be found in the literature [13-16]. The Dahl friction model [14] captures pre-sliding displacement (tissue deformation clearly occurs prior to relative motion between the needle and tissue) and allows to describe friction in the low velocity regimes. Moreover, this model is modified to allow the friction force to be different for different directions of motion and to represent the viscous friction thanks to a viscous damping term. Dahl model is selected to represent friction in this work. It is written as in (3).

$$\frac{df_f}{dx} = \begin{cases} \sigma \left| 1 - \frac{f_f}{D_p} \operatorname{sgn}(\dot{x}) \right|^i \operatorname{sgn}(1 - \frac{f_f}{D_p} \operatorname{sgn}(\dot{x})), & \dot{x} > 0 \\ \sigma \left| 1 - \frac{f_f}{D_n} \operatorname{sgn}(\dot{x}) \right|^i \operatorname{sgn}(1 - \frac{f_f}{D_n} \operatorname{sgn}(\dot{x})), & \dot{x} < 0 \end{cases} \quad (3)$$

with

$$f_f = \int (\frac{df_f}{dx}) dx + b\dot{x} \quad (4)$$

In (3), σ is the slope of the friction curve at $f = 0$ and i is an empirically determined parameter that adjusts the shape of the friction slope function. D_p and D_n are the friction limits in the positive and negative directions, respectively, and b is a viscous damping term. In this work, the Dahl model is simplified using $i=1$. Moreover, with the hypothesis that the velocity is always positive, the model can be written as:

$$\frac{df_f}{dx} = \sigma(1 - \frac{f_f}{D_p}) \quad (5)$$

To obtain a time domain model, it can be observed that:

$$\frac{df_f}{dt} = \frac{df_f}{dx}\frac{dx}{dt} = \sigma(1 - \frac{f_f}{D_p})\dot{x} \quad (6)$$

C. Cutting Force

The cutting force is that which is necessary for the needle tip to slice through the tissue. The used model is based on [6] and this force is given by:

$$f_c = \begin{cases} 0, & x \le d_i, t < t_p \\ c_k, & x > d_i, t \ge t_p \end{cases} \quad (7)$$

where c_k with $k=\{s,f,m,l\}$ is a constant depending of a given tissue (skin, fat, muscle or liver), t is the time and t_p is the time of puncture, d_i is the position of the maximally deformed tissue surface before puncture. The cutting force is supposed to be constant and therefore unrelated to needle depth.

D. Complete Force Model

During the needle insertion phase the complete force model is described by a set of the following disjoint functions:

$$
F=\begin{cases}
0 & x \le d_0 \\
\mu_s x^n & d_0 < x \le d_1 \\
\int (\frac{f_f^s}{dt})dt + b_s \dot{x} + c_s & d_1 < x \le d_2 \\
f_f^s + \mu_f x^n & d_2 < x \le d_3 \\
f_f^s + \int (\frac{f_f^f}{dt})dt + b_f \dot{x} + c_f & d_3 < x \le d_4 \\
f_f^s + f_f^f + \mu_m x^n & d_4 < x \le d_5 \\
f_f^s + f_f^f + \int (\frac{f_f^m}{dt})dt + b_m \dot{x} + c_m & d_5 < x \le d_6 \\
f_f^s + f_f^f + f_f^m + \mu_l x^n & d_6 < x \le d_7 \\
f_f^s + f_f^f + f_f^m + \int (\frac{f_f^l}{dt})dt + b_l \dot{x} + c_l & x > d_7
\end{cases} \qquad (8)
$$

where f_f^s, f_f^f and f_f^m are friction forces of each layer. d_0, d_2, d_4 and d_6 represent the initial position of the skin, the fat, the muscle and the liver, respectively; d_1, d_3, d_5, d_7 are the position of the maximally deformed tissues surface before puncture (see Fig. 1).

As the needle penetrates through the tissue layers, the friction force accumulates [17]. Each tissue has different stiffness and damping coefficients. The different coefficients were assigned to reflect differences in tissues densities.

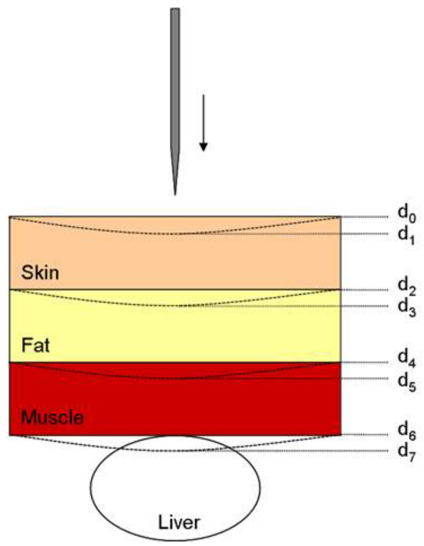

Figure 1. Needle insertion through several tissue layers.

III. SIMULATIONS

Several assumptions have been made regarding the mechanics of needle puncture:

- The puncture force is purely axial along the trajectory of the needle.
- There is no deflection in the needle trajectory as it is inserted.
- Layer puncture force is independent of the initial angle insertion.
- The needle is inserted at a constant velocity until it reaches the target (liver). So, the stiction phenomenon is not considered in this work.
- Withdrawal of the needle is not taken into account.
- The shape effect of the needle tip is not considered.

The complete system dynamics is modeled as a *point-mass dynamics* as follows:

$$
f_u - F(x, \dot{x}) = m\ddot{x} \qquad (9)
$$

where f_u is a control force to be designed to meet particular specifications not defined in this paper, F is the complete force applied on the system and m the total mass including the needle and a robot mechanism that is being built. S*tate variables* are defined by x_1=x, x_2=$\dot{x}$ and x_3=f_f and the corresponding state-space equations are provided as well as the corresponding matrix form. For instance, the dynamics of the skin is given by (10) and (11). Before the skin puncture, the force on the needle is described by the tissue stiffness:

$$
\begin{cases}
\dot{x}_1 = x_2 \\
\dot{x}_2 = \frac{1}{m} f_u - \frac{1}{m}(\mu_s x_1^n) \Rightarrow \\
\dot{x}_3 = 0
\end{cases}
$$

$$
\mathbf{\dot{x}(t)} = \begin{bmatrix} 0 & 1 & 0 \\ -\frac{\mu_s x_1^{n-1}}{m} & 0 & 0 \\ 0 & 0 & 0 \end{bmatrix} \mathbf{x} + \begin{bmatrix} 0 \\ \frac{1}{m} \\ 0 \end{bmatrix} f_u \qquad (10)
$$

The force resulting from needle insertion through the skin is a summation of friction and cutting forces:

$$
\begin{cases}
\dot{x}_1 = x_2 \\
\dot{x}_2 = \frac{1}{m} f_u - \frac{1}{m}(x_3 + c_s) \\
\dot{x}_3 = \sigma(1 - \frac{x_3}{D_p}) x_2 + b_s \dot{x}_2
\end{cases} \Rightarrow
$$

$$
\mathbf{\dot{x}(t)} = \begin{bmatrix} 0 & 1 & 0 \\ 0 & 0 & -\frac{1}{m} \\ 0 & \sigma(1 - \frac{x_3}{D_p}) & -\frac{b_s}{m} \end{bmatrix} \mathbf{x} + \begin{bmatrix} 0 \\ \frac{1}{m} \\ \frac{b_s}{m} \end{bmatrix} f_u + \begin{bmatrix} 0 \\ -\frac{1}{m} \\ -\frac{b_s}{m} \end{bmatrix} c_s \qquad (11)
$$

Simulations have been carried out using Matlab/Simulink. Stiffness coefficients (μ_s, μ_f and μ_m) and damping coefficients (b_s, b_f and b_m) come from [17]; other parameters have been established empirically taking into account some values given in literature. Fig. 2 shows the force profile on the needle during penetration into the skin, the muscle, the fat and the liver at a constant velocity of 3 mm/s. As one would expect, it can be observed four peaks in force after a steady rise, followed by a sharp decrease due to the puncture of the different tissues surfaces (d_1, d_3, d_5 and d_7 represent the position of the needle when it breaks the skin membrane, the fat membrane, the muscle membrane and the hepatic membrane, respectively). The increase in the force is due to penetration through the different layers and the maximum value is reached when the movement ceased (*d=10cm*) in the liver.

IV. CONCLUSION AND FUTURE WORK

This paper introduces a first attempt to model the needle force during the insertion through several tissue layers (skin, fat and muscles) to reach the liver. Our approach is based on the three main force components: stiffness, friction and cutting. Stiffness is modeled by a nonlinear model, friction by a modified Dahl model and cutting by a constant, depending on a given tissue sample. The developed force model can be used in the design of virtual environments for simulation of percutaneous therapies, and the improvement of robot-assisted medical procedures.

Future work will be to define an optimal strategy of control to enhance the puncture task using the dynamic of each layer. Additional research will be necessary to validate the model using experimental data. We are carrying out experiences on a phantom to fit the model with measurements. Another point to develop would be to study the deflections of the needle when it travels through the tissue as well as the effect of velocity, tip type and diameter of the needle.

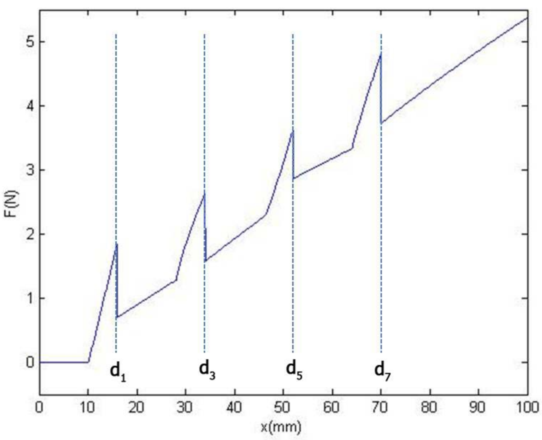

Figure 2. Force on the needle when inserted through the skin, the fat, the muscle and the liver; d_1, d_3, d_5 and d_7 are the positions of the different layers before puncture.

ACKNOWLEDGMENT

The authors wish to thank Dr. John Jairo Martínez Molina for his assistance and advice.

REFERENCES

[1] N. Abolhassani, R. Patel, and M. Moallem, "Needle insertion into soft tissue: a survey", Medical Engineering & Physics, vol. 29, 2007, pp. 413–431.

[2] S. DiMaio, and S. Salcudean, "Needle insertion modeling and simulation", IEEE Transactions on Robotics and Automation, vol. 19, 2003, pp. 864–875.

[3] J. R. Crouch, C. M. Schneider, J. Wainer, and A. M. Okamura, "A velocity-dependent model for needle insertion in soft tissue", in Proceedings of MICCAI , 2005, pp. 624–632.

[4] E. Dehghan, X. Wen, R. Zahiri-Azar, M. Marchal, and S. E. Salcudean, "Parameter identification for a needle-tissue interaction model", in Proceedings of the 29th Annual International Conference of the IEEE EMBS, 2007.

[5] H. Kataoka, T. Washio, K. Chinzei, K. Mizuhara, C Simone, and A. M. Okamura, "Measurement of the tip and friction force acting on a needle during penetration", in Proceedings of MICCAI , 2002, pp. 216–223.

[6] A. Okamura, C. Simone, and M. O'Leary, "Force modeling for needle insertion into soft tissue", IEEE Transactions on Biomedical Engineering, vol. 51, 2004, pp. 1707–1716.

[7] I. Brouwer, J. Ustin, L. Bentley, A. Sherman, N. Dhruv, and F. Tendick, "Measuring in vivo animal soft tissue properties for haptic modeling in surgical simulation", in Proceedings of Medicine Meets Virtual Reality, 2001, pp. 69–74.

[8] J. D. Brown, J. Rosen, Y. S. Kim, L. Chang, M. N. Sinanan, and B. Hannaford, "In-vivo and in-situ compressive properties of porcine abdominal soft tissues", in Proceedings of Medicine Meets Virtual Reality, 2003, pp. 26–32.

[9] B. Maurin, L. Barbé, B. Bayle, P. Zanne, J. Gangloff, M. de Mathelin, A. Gangi, L. Soler, and A. Forgione, "In vivo study of forces during needle insertions", in Scientific Workshop on Medical Robotics, Navigation and Visualization, Remagen, Germany, 2004, pp. 415–422.

[10] L. Barbé, B. Bayle, M. de Mathelin, and A. Gangi, "Needle insertions modeling: identifiability and limitations", Biomedical Signal Processing and Control, vol. 2, 2007, pp. 191–198.

[11] Y.C. Fung, "Biomechanics: Mechanical properties of living tissues", Springer-Verlag, 1993.

[12] M. Heverly, P. Dupont, and J. Triedman, "Trajectory optimization for dynamic needle insertion", in IEEE International Conference on Robotics and Automation, Barcelona, Spain, 2005, pp. 1658–1663.

[13] D. Karnopp, "Computer simulation of slip-stick friction in mechanical dynamic Systems", Journal of Dynamic Systems, Measurement, and Control, vol. 107, 1985, pp. 100–103.

[14] P. Dahl, "Solid friction damping of mechanical vibrations", AIAA Journal, vol. 14, 1976, pp.1675–1682.

[15] P. A. Bliman, and M. Sorine, "Easy-to-use realistic dry friction models for automatic control", Proceedings of 3rd European Conference, Rome, Italy, 1995, pp. 3788–3794.

[16] P. Dupont, B. Armstrong, and V. Hayward, "Elasto-plastic friction model: contact compliance and stiction", in Proc. Amer. Control Conf., Chicago, IL, 2000, pp.1072–77.

[17] O. Gerovichev, P. Marayong, and A. M. Okamura, "The effect of visual and haptic on manual and teleoperated needle insertion", in Proceedings of MICCAI, 2002, pp. 147–154.